E3S Web of Conferences **730**, 01011 (2026)
Soft Soils 2026
https://doi.org/10.1051/e3sconf/202673001011

Critical state characterisation of a natural low-plasticity silt from the Halden NGTS site

Eduardo Parra [1,2*], *Katia* Boschi [3], *Lluís* Monforte [4], *Mohammad* RazaviNasab [1], *Priscilla* Paniagua [5], *Thi Minh Hue* Le [6], *Emir Ahmet* Oguz [5], and *Marcos* Arroyo [4]

[1] Department of Civil and Environmental Engineering, Universitat Politècnica de Catalunya, Barcelona, Spain
[2] Department of Architecture, Construction and Design, Universidad del Bío-bío, Concepción, Chile
[3] Dipartimento di Ingegneria Civile e Ambientale, Politecnico di Milano, Milan, Italy
[4] CIMNE– Universitat Politècnica de Catalunya– BarcelonaTech, Barcelona, Spain
[5] Norwegian Geotechnical Institute, Oslo, Norway
[6] Sweco Norge AS, Trondheim, Norway

Abstract. This paper presents a critical state characterization of a natural low-plasticity silt from the Halden NGTS site (Norway), based on a new laboratory dataset obtained from fully reconstituted loose specimens tested in both drained and undrained triaxial compression over a practical stress range. The results provide a mechanically consistent definition of the Critical State Line (CSL), overcoming limitations associated with existing laboratory data for this deposit, which are largely affected by sampling-induced densification and therefore biased towards denser states. Combining the laboratory-derived CSL with CPT-based interpretation methods, the in-situ state of the Halden silty soil is reassessed. The analysis indicates that the soil is significantly looser than previously inferred from laboratory testing on retrieved samples. This finding has important implications for both the interpretation of historical "intact" laboratory results and the general characterization of transitional silty soils. While the identified loose in-situ state is consistent with a contractive response and potential susceptibility to liquefaction, the main contribution of the study lies in demonstrating the importance of mechanically consistent CSL identification and in highlighting the impact of sampling disturbance on state assessment. Overall, the work provides practical guidance for the reliable characterization of low-plasticity silts within a critical-state framework and supports improved interpretation of both laboratory and in-situ data.

1 Introduction

Low-plasticity loose silts are known to develop high excess pore pressures and pronounced post-peak strength degradation under undrained loading. Such responses have been documented under not only cyclic or seismic excitation, but also monotonic stress paths and during construction-induced disturbances [1-3]. These features place silts among the soils challenging to characterise reliably when instability or liquefaction susceptibility is of concern.

Within the framework of critical state soil mechanics, the critical state line (CSL) and the associated state parameter (i.e. the difference between the current void ratio and the void ratio on the CSL at the same value of mean effective stress; Fig. 1) provide a compact and physically grounded description of whether a soil state is contractive or dilative [4]. This framework underpins both constitutive modelling and CPTu-based interpretation methods for liquefaction susceptibility assessment [3, 5, 6].

However, for silts and transitional soils, CSL identification is often problematic [7]. Compared to clean sands, silts exhibit higher compressibility and greater sensitivity to fabric, drainage conditions, specimen preparation or sampling disturbance, which complicates the experimental identification of critical state conditions [8]. Laboratory tests performed on dense or partially disturbed specimens may not reach true critical state, even at large strains, and may instead converge towards "pseudo"-steady conditions that depend on initial state and stress path [9, 10].

At the Halden NGTS site, this difficulty is compounded by the characteristics of the available laboratory dataset. Existing triaxial results are largely based on specimens that are denser than the estimated in-situ state, consistent with sampling- and handling-induced densification commonly reported for fine-grained and transitional soils [11, 12]. Direct use of such data to infer the CSL may therefore introduce a systematic bias in state parameter estimates, with implications for the interpretation of both laboratory and in-situ test results.

A robust strategy to mitigate these limitations, routinely adopted for tailings characterization [13], relies on fully reconstituted, loose specimens, prepared under controlled conditions to minimise fabric bias and allow systematic exploration of the contractive domain. This approach has been shown to facilitate the attainment of critical state conditions in both drained and undrained triaxial tests, providing a more consistent

* Corresponding author: eduardo.parra@upc.edu

and physically meaningful basis for CSL identification in sands, silty sands and low-plasticity silts [3, 4].

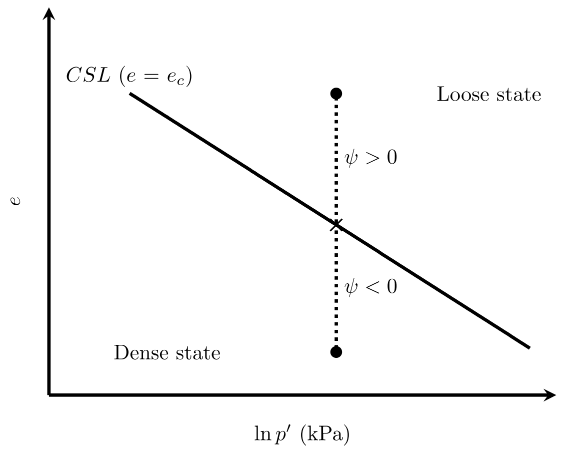

Fig. 1. Schematic representation, in the $e - ln\, p'$ plane, of the CSL and definition of the state parameter.

The specific aim of this study is to propose a representative CSL for the Halden silt by: (i) generating a coherent dataset of drained and undrained triaxial tests on fully reconstituted loose specimens, and (ii) identifying the CSL as a mechanically consistent trend across the dataset. Section 2 describes the Halden NGTS site and the silty soil under exam. Sections 3 to 5 present the experimental programme, the observed mechanical responses, and the resulting CSL identification. Section 6 discusses the implications of the identified CSL for the assessment of in-situ soil state conditions.

2 Halden NGTS site

The Halden site (Fig. 2) is part of the Norwegian GeoTest Sites (NGTS) programme, which was established to provide well-characterised natural soil deposits for the development, validation and benchmarking of geotechnical investigation techniques and interpretation frameworks. NGTS sites have been extensively instrumented and documented, making them particularly suitable for combined in-situ, laboratory and numerical studies of soil behaviour [14].

The Halden deposit includes a thick layer of fjord-marine clayey silt of low plasticity ($PI{\sim}2$), typically considered as normally consolidated, extending approximately from 5 m to 15–16 m depth (saturated weight per unit volume $\gamma{\sim}19$ kN/m^3). Although previous investigations commonly subdivide this layer into Units II and III, these units share a common geological origin and similar index properties. Index and in-situ tests indicate limited plasticity and a transitional mechanical behaviour between sands and clays, including rate-dependent and partially drained responses observed in CPTu testing [15, 16]. A comprehensive description of the geological setting, stratigraphy and available datasets is provided by Blaker et al. [17].

Substantial difficulties in its laboratory characterisation have been documented, primarily related to sampling disturbance and structure-related effects. In Blaker and DeGroot [12], laboratory tests on tube-sampled specimens indicate undrained shear strengths and stiffnesses that are higher than those inferred from in-situ conditions. Consistent with these observations, the triaxial test data available in the NGI database are dominated by samples markedly denser than the estimated in-situ state. The observed scatter in initial void ratio cannot be readily explained by stratigraphic variability within the silty layer and is instead consistent with sampling-induced densification effects. As a consequence, while the existing laboratory datasets provide valuable insight into the general stress–strain behaviour of the Halden silt, their direct use for critical state characterisation is problematic. In particular, the dense initial states of the tested specimens limit the ability to reach true critical state conditions during shearing and may lead to the identification of “pseudo”-steady states rather than representative critical states [9, 10].

Fig. 2. (a) Location map and (b) aerial view of the Halden NGTS test site.

3 Experimental campaign

The experimental programme to identify the critical state line of the Halden silt, followed what is now a well-honed methodology for human-made silts (i.e. tailings) in which CSL are interpreted from the results of a suite of undrained and drained triaxial tests on loose reconstituted specimens [3, 7, 13]. The material used for laboratory testing was retrieved by standard tube sampling at the Halden NGTS site, at coordinates 6555907.05 N and 635289.23 E (EUREF89). A tube section spanning depths between 10 and 11 m was selected, from which fully reconstituted specimens were prepared for triaxial testing, in general accordance with UNE-EN ISO 17892-9 (2019), ASTM D7181-20 (2020) and ASTM D4767-11 (2020).

The use of fully reconstituted specimens limits the variability induced by sampling disturbance, fabric alteration and inadvertent densification associated with tube sampling and handling. These effects are known to significantly bias laboratory-derived parameters in low-plasticity silts when undisturbed specimens are used [8].

Previous laboratory investigations on Halden silt had also noted the pronounced sensitivity of this material to drainage conditions and procedural details. Particular care was therefore devoted to specimen preparation, saturation and consolidation. Specimens (140 mm high and 70 mm in diameter) were prepared under loose conditions by static compaction. For the Halden silt ($G_s = 2.61$, $e_{max} = 1.27$, $e_{min} = 0.58$), a target initial void ratio of approximately $e_0 \simeq 1.0$ was selected, corresponding to a relative density of about $D_r \simeq 40\%$ and clearly within the contractive domain. This choice is consistent with established recommendations for critical state testing, which discourage the use of dense specimens due to their tendency to develop strain localisation and non-uniform deformation [18, 19].

Material extracted from the sampling tube was oven-dried at 110 °C and gently disaggregated. Distilled water was then added to achieve a target water content of approximately 12–13%. After a resting period exceeding 16 h to ensure moisture homogenisation, specimens were formed in a mould using controlled static compaction in two equal-volume layers, allowing a reproducible void ratio to be obtained. The mould was subsequently removed and the specimen mounted on the triaxial pedestal.

Both drained (DCTXT) and undrained (UCTXT) isotropically consolidated standard triaxial compression tests were performed. The complete testing programme, including drainage conditions and imposed confining pressure p'_c values, is summarised in Table 1.

Saturation was achieved using the water percolation method, maintaining a constant pressure differential between cell and back pressure while progressively increasing both pressures in ramps. A high back pressure of 700 kPa was applied and maintained overnight to eliminate residual air. All specimens achieved Skempton B-values ≥ 0.96 prior to consolidation.

Table 1. Laboratory test program.

Test ID	Test type	p'_c [kPa]
U100	UCTXT	100
U150	UCTXT	150
U200	UCTXT	200
D100	DCTXT	100
D200	DCTXT	200

Following saturation, specimens were isotropically consolidated to the target mean effective stress p'_c. The imposed p'_c values were selected to represent stress levels relevant to the in-situ conditions at the Halden site and to practical geotechnical applications.

Shearing was then performed under displacement control, at an axial strain rate of 0.67 %/min for undrained tests, 0.11 %/min for the D100 test and 0.06 %/min for the D200 test. The strain rate for the D200 test was reduced following evidence of transient pore-pressure response (i.e. incomplete drainage) during D100, in order to ensure fully drained conditions.

Stress measurements were corrected for membrane resistance and changes in specimen area in accordance with ASTM standards.

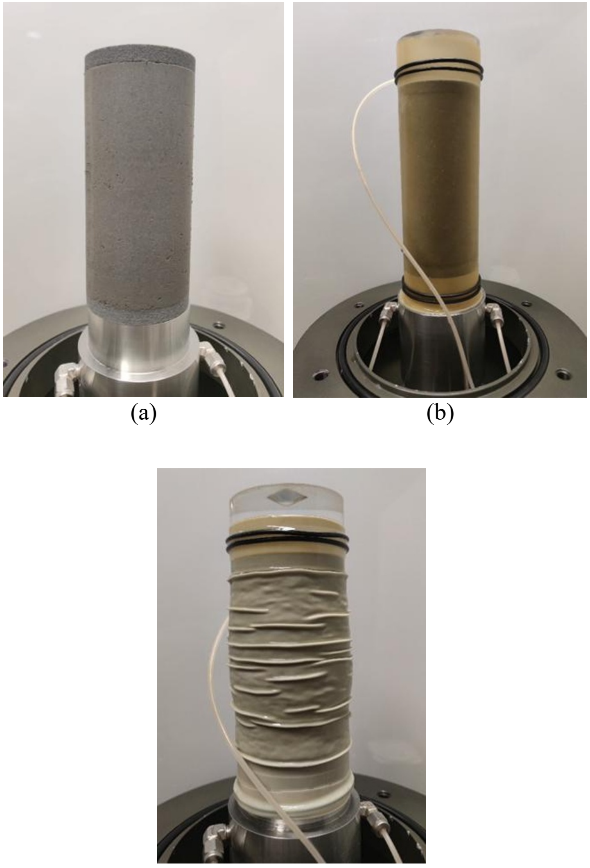

(a) (b) (c)

Fig. 3. Fully reconstituted triaxial specimen: (a) without membrane, (b) before and (c) after D200 shearing (p'_c = 200 kPa).

All specimens were sheared to large axial strains, within the limits imposed by the apparatus (20%). Consistent with the loose initial state, deformation remained diffuse and manifested as a barrelling-type pattern, with no evidence of strain localisation or shear band formation (Fig. 3).

One of the main practical issues encountered during testing concerned the “docking” stage prior to consolidation. A small axial load of 10 kPa is commonly applied to keep the specimen in position and enable reliable measurements of axial strain. However, due to the very loose state of the material, this load caused collapse of several specimens. Consolidation was therefore performed without any docking load. Once consolidation was completed, and the specimens had gained sufficient stiffness at the target effective pressures, a docking load of 10 kPa was applied prior to shearing.

Further details on specimen preparation, testing procedures and quality control measures are documented in Boschi et al. [20] and Parra [21].

4 Triaxial test results

This section presents the results of the drained and undrained triaxial compression tests performed on the fully reconstituted Halden silt specimens. The focus is placed on the effective stress paths (Fig. 4), the stress ratio–strain response (Fig. 5a) and the $e - \log p'$ trajectories (Fig. 5b) relevant to the identification of critical-state conditions.

Fig. 4a shows the effective stress paths of all triaxial compression tests in the $q - p'$ (deviatoric versus mean effective stress) plane. The shearing paths shown originate from q = 10 kPa, corresponding to the applied docking load.

The undrained tests exhibit predominantly contractive stress paths, with a clear tendency for p' to decrease during shearing as excess pore pressures develop, resulting in limited mobilisation of deviatoric stresses compared with the drained responses. Overall, these stress paths highlight the strong influence of drainage conditions and confirm the expected increase in mobilised strength with increasing initial effective stress level. The D100 test departs slightly from fully drained paths at the start of shearing, suggesting that fully drained conditions may not have been achieved initially (transient pore-pressure build-up) before the response transitions to the expected drained behaviour.

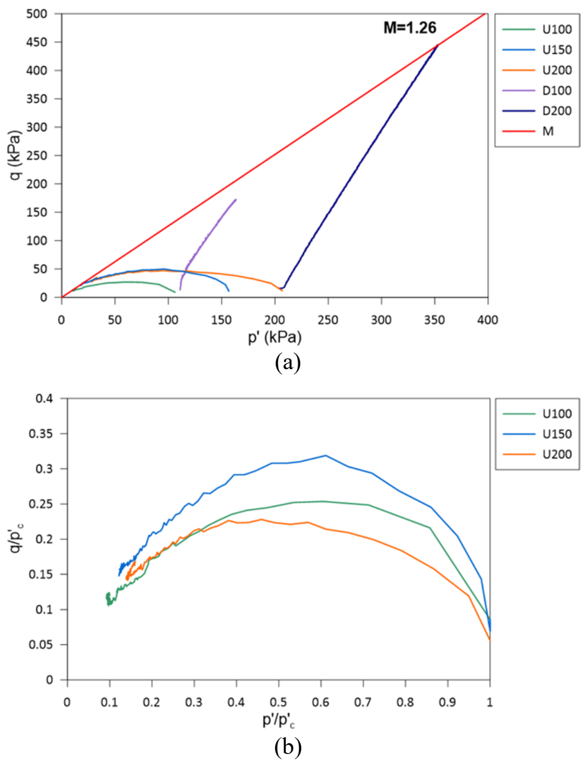

Fig. 4. (a) Stress paths of all triaxial tests in the $q - p'$ plane; (b) normalised paths of the undrained tests, expressed as q/p'_c versus p'/p'_c.

Despite differences in the initial p'_c, the undrained stress paths show a similar overall evolution. This behaviour is shown in normalised form in Fig. 4b, where the undrained stress paths are scaled by the initial mean effective stress (q/p'_c versus p'/p'_c). Unexpectedly, the U200 test remains consistently below the other undrained tests in terms of q/p'_c, suggesting some uncontrolled procedural anomaly might be affecting the result.

The stress–strain response of both drained and undrained tests is shown in Fig. 5a, expressed in terms of stress ratio $\eta = q/p'$ versus axial strain ε_a. All specimens were sheared to large axial strains, and no peak strength or softening was observed. Instead, the response is characterised by gradual mobilisation of shear resistance and the attainment of approximately constant stress ratios at large strains, consistent with diffuse deformation under loose conditions.

The volumetric response of the drained tests is highlighted in Fig. 5b, which shows void ratio evolutions of all the performed tests in the $e - log\, p'$ plane during both isotropic compression and subsequent shearing. The initial void ratios e_0 of the drained triaxial tests were adjusted to ensure that specimens consolidated at the same p'_c value start from a common initial void ratio. The applied corrections were limited in magnitude (+0.02 for D100 and −0.02 for D200). Such adjustments reflect the well-known experimental difficulties associated with the accurate determination of e_0 in laboratory testing, particularly for fine-grained and transitional soils [7].

During shearing, the specimens exhibit contractive behaviour over the entire stress range explored. The drained trajectories are sub-parallel, indicating a similar compressibility response across the investigated stress levels.

Taken together, the drained and undrained results indicate a consistent mechanical response across the test series. While individual experiments are affected by small minor anomalies, the overall dataset provides sufficient coverage and coherence to support a representative critical-state interpretation. Compared to previously available laboratory data dominated by denser, disturbance-affected specimens, the present results offer a clearer basis for defining the CSL of the Halden silt.

5 Identification of the CSL

The drained and undrained triaxial test results define a mechanically coherent dataset compatible with the existence of a unique critical state line for the reconstituted Halden silt. Recent inverse and Bayesian calibration studies have shown that, for loose and normally consolidated soils, a limited number of carefully selected and mechanically consistent triaxial tests can be sufficient to identify reliable CSL parameters, and that increasing the size of the experimental dataset does not necessarily improve CSL definition when defective or anomalous additional tests are included [22, 23]. In this context, the dataset presented herein is considered sufficient to identify a representative CSL for the Halden silt, as it spans both drained and undrained conditions and exhibits consistent large-strain responses under diffuse deformation.

Despite differences in drainage conditions and initial mean effective stress, all the specimens converge towards a stable stress ratio at large strain in Fig. 5a. This convergence indicates the attainment of steady shearing conditions and supports the identification of a representative critical stress ratio M, which characterises the CSL in stress space according to

$$q = M\,p' = 1.26\,p' \qquad (1)$$

In calibrating the M value (corresponding to $\phi' = 31°$), greater confidence was placed on the stress ratios mobilised in the U100, U150 and D200 tests, which converge towards essentially the same q/p' plateau under steady shearing conditions. These tests provide the most reliable basis for identifying the critical stress ratio. Less weight was given in this respect to tests D100 (sheared too fast and hence not reliably drained) and U200 (anomalous normalized response).

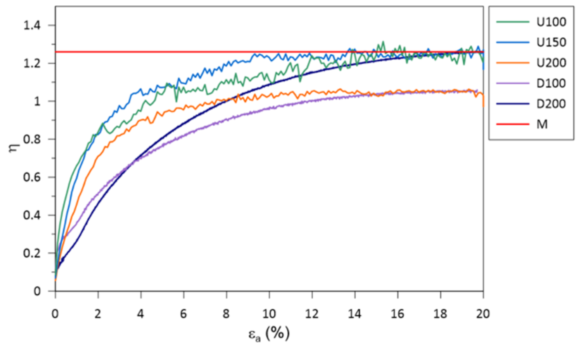

(a)

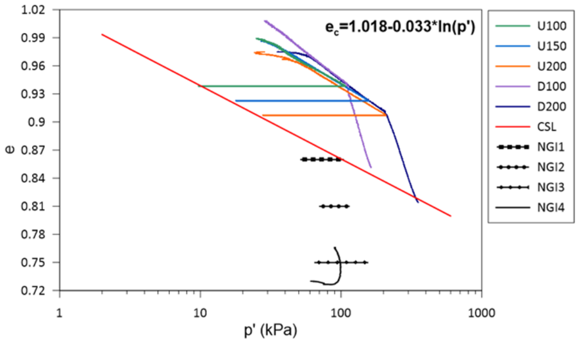

(b)

Fig. 5. (a) Stress ratio $\eta = q/p'$ versus axial strain ε_a for drained and undrained triaxial tests; (b) void ratio e versus mean effective stress p' ($\log_{10}$ scale), showing the inferred Critical State Line (CSL). TXT paths from the NGI database are also shown for comparison (black lines).

An analogous interpretation effort was carried out to identify the CSL in the $e - \ln p'$ plane. It is well known that the CSL in the $e - \ln p'$ plane is not strictly linear when a sufficiently wide range of mean effective stresses is explored, with systematic departures from linearity reported for sands and transitional soils at low and high stress levels [24]. Nevertheless, for the stress interval investigated in the present study a linear representation of the CSL was considered adequate and the data obtained (Fig. 5b) supported this approach.

Over the investigated stress range, the CSL was thus approximated by a straight line of the following form

$$e_c = \Gamma - \lambda \ln p' = 1.018 - 0.033 \ln p' \qquad (2)$$

where Γ is the void ratio at a reference mean effective stress of p'= 1 kPa and λ is the slope of the CSL in the $e - \ln p'$ plane. Again, while fitting parameters Γ and λ more weight was given to the most reliable tests (U100, U150 and D200). Overall, the scatter of the dataset is limited, and the resulting trend is coherent and physically meaningful. The calibrated CSL parameters obtained for Halden are consistent with values reported in the literature for low-plasticity silts [7, 25, 26], which supports the plausibility of the identified CSL.

6 Critical state line as a reference for in-situ state assessment

Building on this basis, the laboratory-derived CSL was used as a reference framework to explore the in-situ state of the silty layer at the Halden NGTS. Cone penetration test CPTu data collected within the G-SCAN project [20] (employed test ID: HALC639) were indeed employed to derive in-situ estimates of state parameter ψ. The interpretation followed the procedure proposed by Plewes et al. [27]. In this application, the method was implemented by directly adopting the M and λ values obtained from the laboratory-derived CSL, rather than relying on empirical correlations between friction and compressibility. For the in-situ stress state, over-consolidation ratio $OCR = 1$ was assumed, and at-rest lateral earth pressure coefficient K_0 was estimated using Jaky's formula.

The results of the Plewes method for the Halden site are shown as a profile of ψ along the layer depth in Fig. 6. The predominantly positive values of ψ within the silty layer indicate a contractive response under undrained loading and, according to common interpretation, a potentially in-situ liquefiable condition. The Plewes method is commonly adopted as a screening approach for state assessment of tailings and, while it is known to exhibit substantial variability at a given depth within a single site, it is generally believed to be approximately unbiased when results are compared across multiple sites. In this sense, the method is regarded as correct on average, particularly when, as done here, site-specific CSL values are incorporated into the analysis [13].

By combining the CPT-derived estimates of ψ with the CSL identified in this study, a representative range of in-situ void ratios was back-calculated for the silty layer, leading to values of e approximately between 0.9 and 1.0 (vertical profile of e along depth in Fig. 7). The same figure also compares the back-calculated profile with the void ratios measured on retrieved samples [17] and the initial void ratios of the reconstituted specimens tested in this study.

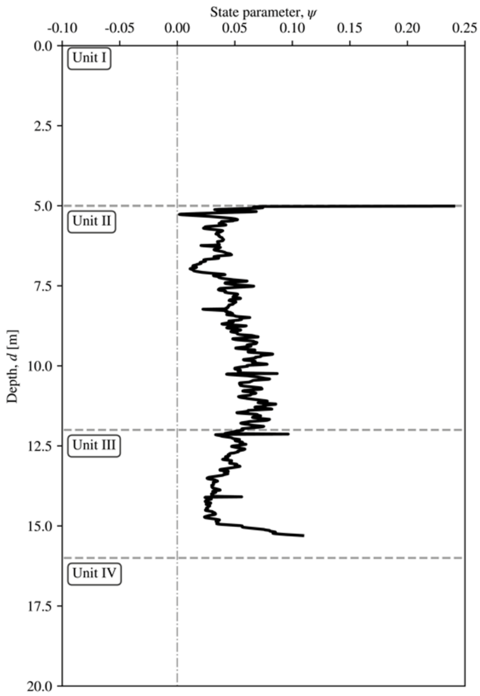

Fig. 6. Derived vertical profile of ψ along depth d.

The in-situ-derived void ratios are systematically higher than those measured on the retrieved samples, as well as than the initial void ratios of triaxial specimens available in the NGI laboratory database for the same soil layer (a selection of which is shown in Fig. 5b). This result is consistent with systematic observations of sampling induced densification in silty tailings [11, 13].

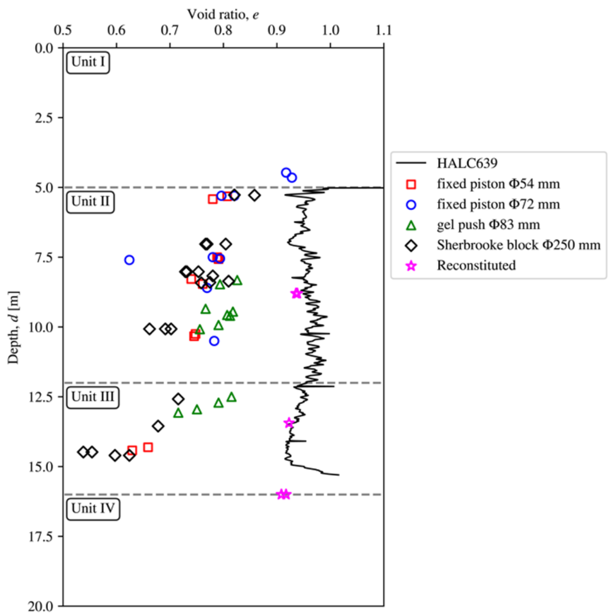

Fig. 7. Derived vertical profile of e along depth d.

While the void ratios obtained from retrieved samples exhibit substantial scatter, the CPT-based back-calculated profile appears comparatively uniform with depth. This apparent homogeneity likely reflects relatively uniform in-situ soil conditions, notwithstanding the fact that CPTu readings are not strictly point measurements but represent a spatially averaged soil response over a finite zone surrounding the cone tip [28, 29].

Despite these limitations, the combined interpretation yields two relevant insights. First, it highlights the role of a mechanically consistent CSL as a reference framework: without it, CPT-based estimates of state parameter and in-situ void ratio would remain weakly constrained and largely reliant on empirical correlations. Second, the comparison suggests that many laboratory specimens referred to this site were tested at void ratios lower than those representatives of the in-situ soil state, consistent with systematic densification effects induced by sampling and handling in low-plasticity silts.

7 Conclusion

This study establishes a mechanically consistent critical state line for the Halden NGTS low-plasticity silt, identified from drained and undrained triaxial tests on fully reconstituted loose specimens. The CSL is defined coherently in both the $q - p'$ plane, through a critical stress ratio M, and in the $e - \ln p'$ plane over the investigated stress range.

The results highlight the importance of a careful and critical evaluation of the CSL in transitional soils. Given the widespread use of critical-state-based frameworks in design and interpretation, the CSL should be regarded as a design-relevant parameter rather than a purely descriptive one. Consequently, robust CSL identification, grounded in mechanically consistent laboratory evidence, is essential to support reliable engineering decisions. The benefits of this approach are already widely recognized in tailings engineering; the example of Halden illustrated in this work makes the case for extending that approach also to the characterization of natural silts.

The authors gratefully acknowledge that this work is part of the G-SCAN – Geotechnical Soil Characterization to Alleviate Natural Disasters project, funded within the framework of GEOLAB – Science for Enhancing Europe's Critical Infrastructure under the European Union's Horizon 2020 Research and Innovation Programme. The authors express their gratitude to NGTS - Norwegian Geo-Test Sites team for making background data and reports accessible.

References

1. P. V. Lade, J. A. Yamamuro, Effects of nonplastic fines on static liquefaction of sands. Can. Geotech. J. **34**, 918–928 (1997). https://doi.org/10.1139/t97-052
2. S. M. Olson, T. D. Stark, Yield strength ratio and liquefaction analysis of slopes and embankments. J. Geotech. Geoenviron. Eng. **129**(8), 727-737 (2003). https://doi.org/10.1061/(ASCE)1090-0241(2003)129:8(727)
3. M. G. Jefferies, K. Been, Soil Liquefaction: A Critical State Approach, 2nd ed. CRC Press, London (2016).
4. K. Been, M. G. Jefferies, A state parameter for sands. Géotechnique **35**, 99–112 (1985). https://doi.org/10.1680/geot.1985.35.2.99

5. R. W. Boulanger, I. M. Idriss, CPT-based liquefaction triggering procedure, J. Geotech. Geoenviron. Eng. **142**(2) (2016) 04015065. https://doi.org/10.1061/(ASCE)GT.1943-5606.0001388
6. L. Monforte, M. Arroyo, A. Gens, A relation between undrained CPTu results and the state parameter for liquefiable soils. Can. Geotech. J. **60**.11 (2023): 1756-1774. https://doi.org/10.1139/cgj-2022-0377
7. D. Reid, A. Fourie, J. L. Ayala, S. Dickinson, F. Ochoa-Cornejo, R. Fanni, G. Suazo, Results of a critical state line testing round robin programme. Géotechnique **71**, 616–630 (2021). https://doi.org/10.1680/jgeot.19.P.373
8. R. Carroll, M. Long, Sample disturbance effects in silt, J. Geotech. Geoenviron. Eng. **143**(9) (2017) 0401706. https://doi.org/10.1061/(ASCE)GT.1943-5606.0001749
9. J. A. Sladen, R. D'Hollander, E. L. Krahn, The liquefaction of sands: a collapse surface approach. Can. Geotech. J. **22**, 564–578 (1985). https://doi.org/10.1139/t85-076
10. K. Been, M. G. Jefferies, J. Hachey, The critical state of sands. Géotechnique **41**, 365–381 (1991). https://doi.org/10.1680/geot.1991.41.3.365
11. K. Been Characterizing mine tailings for geotechnical design. Austr. Geomech. **51**(4), 59-78 (2016).
12. Ø. Blaker, D. J. DeGroot, Intact, disturbed, and reconstituted undrained shear behavior of low-plasticity natural silt, J. Geotech. Geoenviron. Eng. **146**(8) (2020) 04020062. https://doi.org/10.1061/(ASCE)GT.1943-5606.0002299
13. A. Fourie, R. Verdugo, A. Bjelkevik, L. A. Torres-Cruz, D. Znidarcic, Geotechnics of mine tailings: a 2022 State of the art. Proc. 20th ICSMGE **20**, 121–183 (2022).
14. J. S. L'Heureux, T. Lunne, Characterization and engineering properties of natural soils used for geotesting. AIMS Geosci. **6**, 35–53 (2020). https://doi.org/10.3934/geosci.2020004
15. R. Carroll, P. Paniagua, Variable rate of penetration and dissipation test results in a natural silty soil, in: Cone Penetration Testing **2018**, CRC Press, London (2018) 205–212.
16. P. Carotenuto, C. Bilici, T. Lunne, A. H. Augustesen, L. Krogh, H. Dias, N. Adams, Study of partial drainage effects in a natural silty deposit using variable rate CPTu testing. Offshore Site Investig. Geotech. – Proc. 9th Int. Conf., Soc. Underw. Technol., London **2023** (2023), 305–312.
17. Ø. Blaker, R. Carroll, A. P. Paniagua Lopez, D. J. DeGroot, J. S. L'Heureux, Halden research site: geotechnical characterization of a post glacial silt, AIMS Geosci. **5**(2) (2019) 184–201. https://doi.org/10.3934/geosci.2019.2.184
18. J. Desrues, R. Chambon, M. Mokni, F. Mazerolle, Void ratio evolution inside shear bands in triaxial sand specimens studied by computed tomography. Géotechnique **46** (3), 529–546 (1996). https://doi.org/10.1680/geot.1996.46.3.529
19. A. Viana Da Fonseca, D. Cordeiro, and F. Molina-Gómez, Recommended Procedures to Assess Critical State Locus from Triaxial Tests in Cohesionless Remoulded Samples, Geotechnics **1**, 95–127 (2021). https://doi.org/10.3390/geotechnics1010006
20. K. Boschi, E. Parra, L. Monforte, P. Paniagua, E.A. Oguz, M. Arroyo, GEOLAB – G-SCAN – Geotechnical Soil Characterization to Alleviate Natural Disasters. Zenodo (2025). https://doi.org/10.5281/zenodo.15024434
21. E. Parra. MSc thesis: Determination of the Critical State Line for a Silty Soil from Halden, Norway. Universitat Politècnica de Catalunya (2025)
22. M. Arroyo, L. Monforte, S. Collico, How many triaxial tests do you actually need to get a critical state line? Proc. Tailings Mine Waste **2024**, 2191–2202 (2024).
23. L. Monforte, S. Collico, M. Arroyo, Bayesian identification of the critical state line of a liquefiable silt. Manuscript submitted for publication (2026).
24. X.S. Li, Y. Wang. Linear Representation of Steady-State Line for Sand. J. Geotech. Geoenviron. Eng. **124**, 1215–1217 (1998).
25. D. D. Porcino, V. Diano, T. Triantafyllidis, & T. Wichtmann. Predicting undrained static response of sand with non-plastic fines in terms of equivalent granular state parameter. Acta Geotech. **15**(4), 867-882, (2020).
26. J. Ayala, A. Fourie, & D. Reid. Improved cone penetration test predictions of the state parameter of loose mine tailings. Can. Geotech. J. **59**(11), 1969-1980, (2022). https://doi.org/10.1139/cgj-2021-0460
27. H.D. Plewes, M.P. Davies, & M. Jefferies, CPT based screening procedure for evaluating liquefaction susceptibility. Proc. 45th Can. Geotech. Conf., Toronto, Canada **45** (1992).
28. Boulanger, R.W. DeJong, J.T. Inverse filtering procedure to correct cone penetration data for thin-layer and transition effects. Cone Penetration Testing **2018** (2018).
29. Monforte, L., Collico, S. Inherent and CPTu-measured scale of fluctuation of undrained geomaterials: a numerical perspective. Proc. 7th Int. Conf. Geotech. Geophys. Site Charact. **2024** (2024).